White paper

HD FOV 4.0

Technical principles and phantom measurements evaluating HU accuracy and skin-line accuracy in the extended field of view (FOV) region for VB10, version 4.0

Matthias Baer, PhD, Siemens Healthineers AG
Harald Schoendube, PhD, Siemens Healthineers AG

SIEMENS Healthineers

Introduction

Accuracy of dose calculation in radiotherapy often depends on precise assignment of the electron density to each voxel in an image, and on precise reconstruction of patient geometry. Imaging is typically carried out on a CT simulator (a CT scanner that can be used for treatment simulation and has features that support radiotherapy) that has a wide bore (typically at least 80 cm) to accommodate bariatric cases, immobilization devices, patient positioning systems, etc.

The CT simulator typically has a scan field of view (sFOV) of 50–60 cm, and in most cases the patient boundary is well within the sFOV. However, in certain cases – for example, in patients with higher BMI or when using a positioning device such as a breast board – part of the patient's anatomy extends beyond the sFOV. The limited data in the regions outside the sFOV often lead to inaccurate patient geometry and reduced accuracy on the HU in the extended FOV region.

To overcome this, extended FOV algorithms[1,2] have been developed and constantly improved over the years to increase the accuracy of reconstruction outside the sFOV. In this white paper, we describe our implementation of the extended FOV reconstruction algorithm HD FOV 4.0. Furthermore, we demonstrate HU and geometric accuracy in the extended FOV region using phantom studies.

Contents

Theory

The current implementation of the HD FOV 4.0 algorithm consists of several steps to reduce artifacts in the regions outside the sFOV. These include: a) mass-conserving boundary estimation, b) sinogram estimation, and c) artifact reduction, all shown in Figure 1.

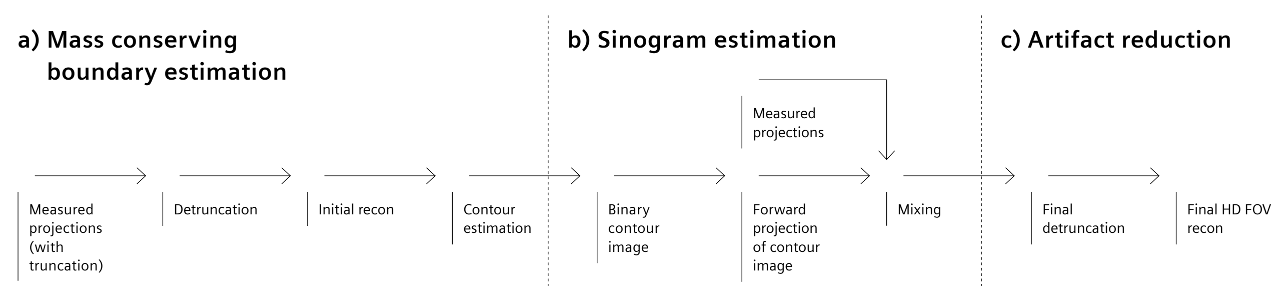

Figure 1: Flowchart for the HD FOV 4.0 algorithm showing the three main steps: mass-conserving boundary estimation, sinogram estimation, and final artifact reduction.

Mass-conserving boundary estimation

To reconstruct information in the extended FOV region, one needs to start with an estimate of the patient boundary from the limited data available. In our implementation, we start with the assumption that every projection that covers the entire object/patient should result in a constant mass. When the object or patient being imaged lies at least partly outside the sFOV, this condition is violated and the data for those projections are truncated during measurements, as seen on the left in Figure 2. The projection mass defined as the normalized cumulative sum of the attenuation values of a projection varies as a function of the angle (0°–360°). The normalized projection mass is 1 for projection angles that see the entire object/patient, and lower in other cases.

To detruncate the data, a mass consistency condition is applied and an initial estimate of projections is created so that the mass is identical in all the projections (Figure 2). Extrapolation is carried out in projection space for the truncated projections using a cosine-shaped function so that the mass is consistent across all the projections. To avoid any artifacts from an abrupt transition from measured data to extrapolated data, the algorithm ensures that the transition between measured and extrapolated data is smooth.

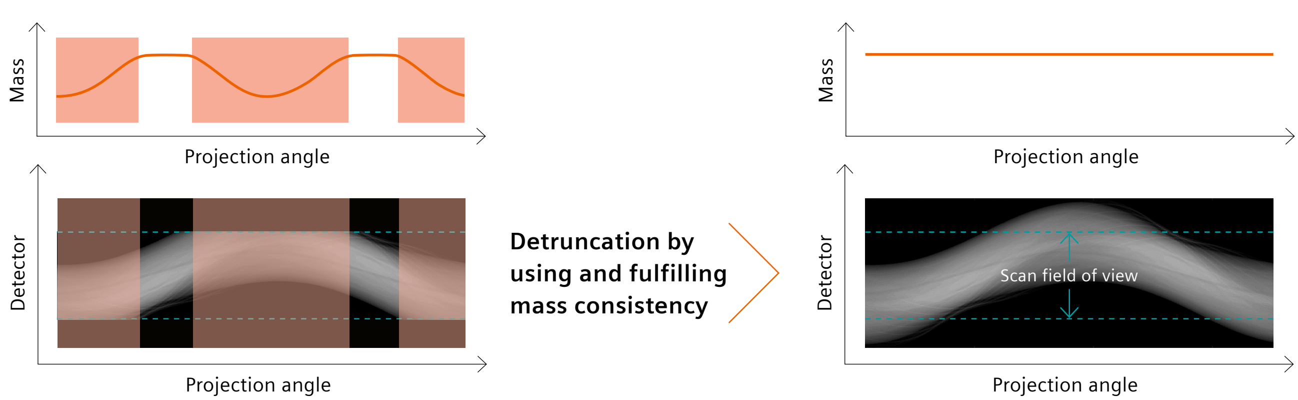

Figure 2: HD FOV 4.0 uses a data extrapolation based on the mass conservation principle in order to detruncate the measured CT data.

An initial estimate of the image is reconstructed (Figure 3) using these extrapolated projections. Based on this reconstruction, a refined estimation of the parts of the patient lying outside the sFOV is performed. To do so, the initial reconstruction of the object (after applying the mass-conserving data estimation) is first binarized to get an approximation of the boundaries. For a more reliable and more stable estimate of the patient boundary, a three-dimensional low-pass filter is applied to the initial reconstruction prior to thresholding. The application of this filter helps reduce the sensitivity of binarization with respect to artifacts and finally leads to a more continuous estimate of the patient boundaries.

Sinogram estimation and artifact reduction

The measured data is now extrapolated and mixed with the forward projections from the binary patient contour (Figure 1, Figure 3). This step can potentially result in a final image that is a close representation of the patient being imaged. However, this is only true when the truncation in the measured data is fully captured in the binary patient contour image. Structures that are not covered by the binary patient contour image may still cause truncation artifacts; to remove these, a final detruncation step is carried out in the projection space. As a last step, the final image is reconstructed from the detruncated projections.

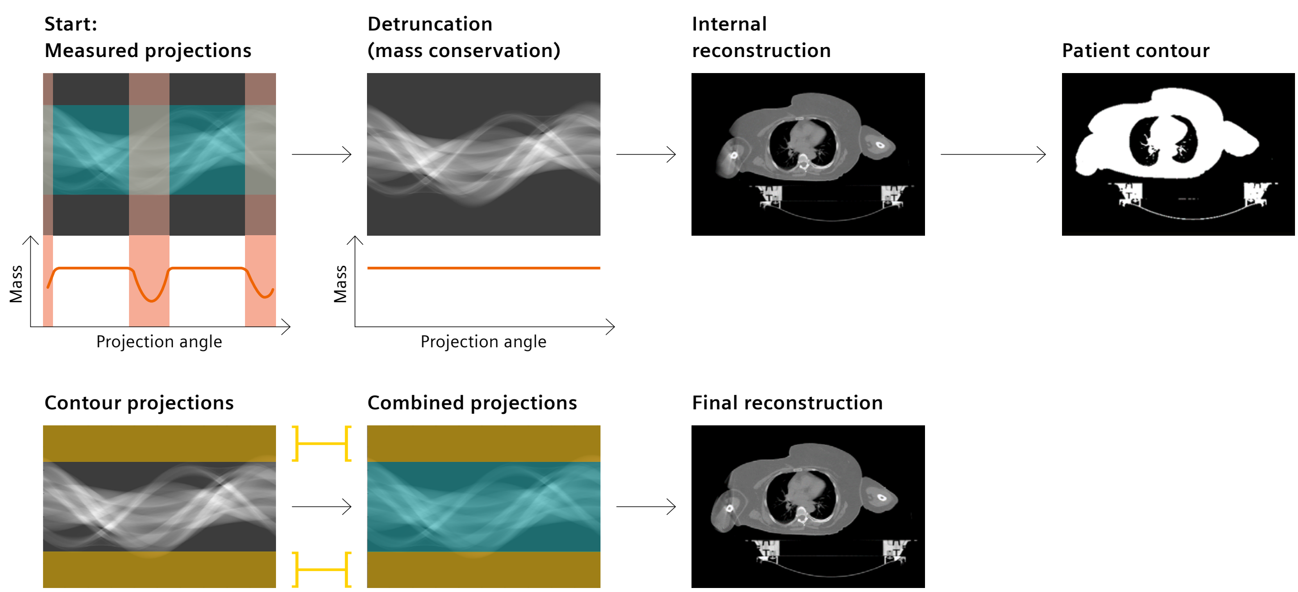

Figure 3: Flowchart of the HD FOV 4.0 algorithm. Starting with the truncated projection data, an initial reconstruction is performed after detruncation using the principle of mass conservation. From this initial reconstruction, a "patient contour image" is computed by thresholding. The binary patient contour is then forward projected, and the forward projections of the patient contour image are used to extrapolate the initial measured projection data. Note that the measured data (green shading) is not altered by this extrapolation. After applying a final detruncation, the final image is reconstructed from the extrapolated projections.

Phantom studies

To evaluate the performance of the HD FOV 4.0 algorithm, we set up a study using a Gammex electron density phantom with a 330 mm diameter (Gammex, Middleton, WI, USA). The images were acquired on a diagnostic CT scanner with a 70 cm bore (SOMATOM go.Up), on the diagnostic 82-cm-bore CT scanners SOMATOM X.cite and NAEOTOM Alpha, and on an 85-cm-bore CT scanner (SOMATOM go.Open Pro) designed for radiotherapy. The phantom was imaged in three different positions in the scanner as shown in Figure 4. For the first position, the phantom was completely contained within the sFOV. For the second and third positions, the height was adjusted so that parts of the phantom were located outside the sFOV of the CT scanner. The absolute phantom positions were adjusted for the different geometries of the investigated CT scanners. Images were reconstructed using an FOV of 700 mm on the 70-cm-bore CT scanner. The reconstructed FOV was set to 815 mm on the 82 cm scanners, and to 850 mm on the 85 cm scanner. An overview of the phantom positions, reconstructed FOVs, and sFOVs is given in Table 1 (see also Figure 4, Figure 6, and Figure 7). Note that in the case of NAEOTOM Alpha, which is equipped with a photon-counting detector, the applicability of HD FOV 4.0 is limited to T3D reconstructions, which are non-spectral reconstructions that use only the data from the lower T1 threshold of the quantum counting detector.

CT Scanner	Position 1	Position 2	Position 3	Reconstructed FOV	Scan field of view (sFOV)
SOMATOM go.Up	Within sFOV	Outer phantom edge at 580 mm	Outer phantom edge at 680 mm	700 mm	500 mm
SOMATOM X.cite	Within sFOV	Outer phantom edge at 630 mm	Outer phantom edge at 750 mm	815 mm	500 mm
NAEOTOM Alpha	Within sFOV	Outer phantom edge at 630 mm	Outer phantom edge at 750 mm	815 mm	500 mm
SOMATOM go.Open Pro	Within sFOV	Outer phantom edge at 740 mm	Outer phantom edge at 810 mm	850 mm	600 mm

Table 1: Positions of the Gammex phantom that were used on the different scanners to evaluate HD FOV 4.0

HU accuracy

HU accuracy in the extended FOV region was evaluated by measuring the mean HU value in a region of interest (ROI). An ROI was placed at the 12 o'clock position within the Gammex phantom, as indicated by the yellow circle in Figure 4, Figure 6, and Figure 7. This measurement was repeated on six central slices, and the average value over all slices was computed. The mean HU value within the ROI was compared to a reference mean HU value from the ROI in the case where the phantom is contained within the sFOV (left image in Figure 4, Figure 6, and Figure 7).

Phantom diameter accuracy

Diameter accuracy was evaluated by measuring 75 line profiles distributed in equally spaced angle increments within the yellow shaded area (some example lines are plotted in Figure 5). The angle range for the line profiles was chosen so that the whole range of truncation is approximately covered for the second phantom position, as shown by the yellow shaded region in Figure 5, Figure 6, and Figure 7.

The full width at half maximum (FWHM) of the 75 line profiles was computed for the six central image slices of the reconstruction. The reported diameter is the FWHM averaged over all 75 line profiles and all slices. As for the evaluation of the HU values, the case where the entire phantom is contained within the sFOV was used as reference (left image in Figure 5, Figure 6, and Figure 7).

The datasheet value for the diameter of the Gammex phantom[3] is 330 mm.

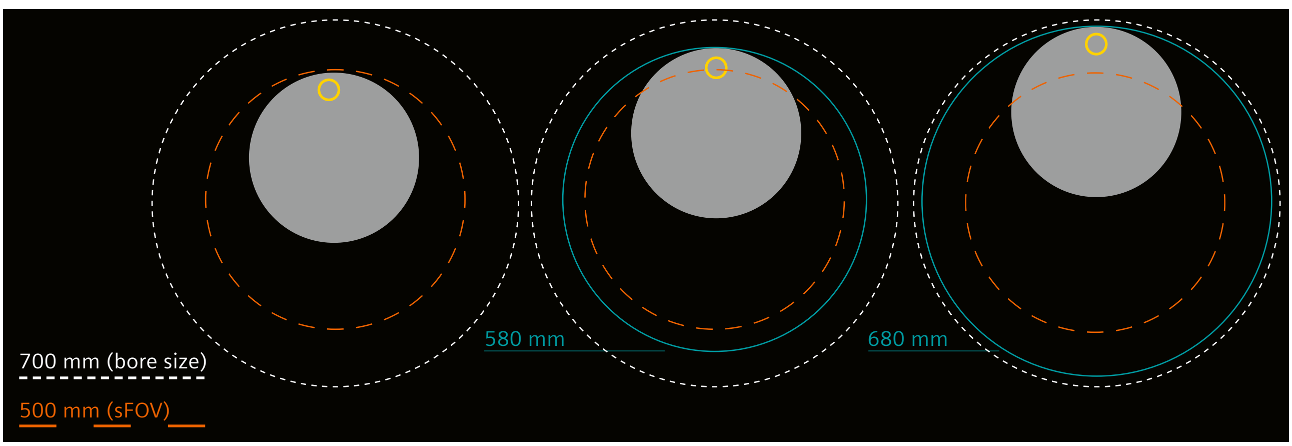

Figure 4: Setup for imaging the Gammex phantom at three different heights on the 70-cm-bore CT scanner SOMATOM go.Up. From left to right: phantom completely in the sFOV, outer phantom edge at 580 mm, and outer phantom edge at 680 mm.

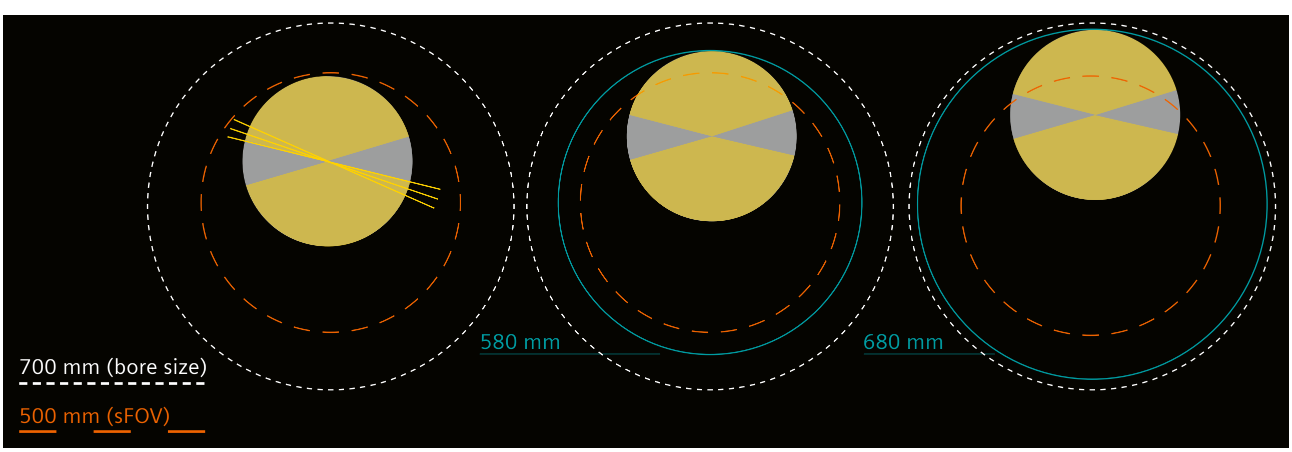

Figure 5: Setup to measure diameter accuracy on the 70-cm-bore CT scanner SOMATOM go.Up. The 75 line profiles in the six central slices were used to report the accuracy of the phantom diameter.

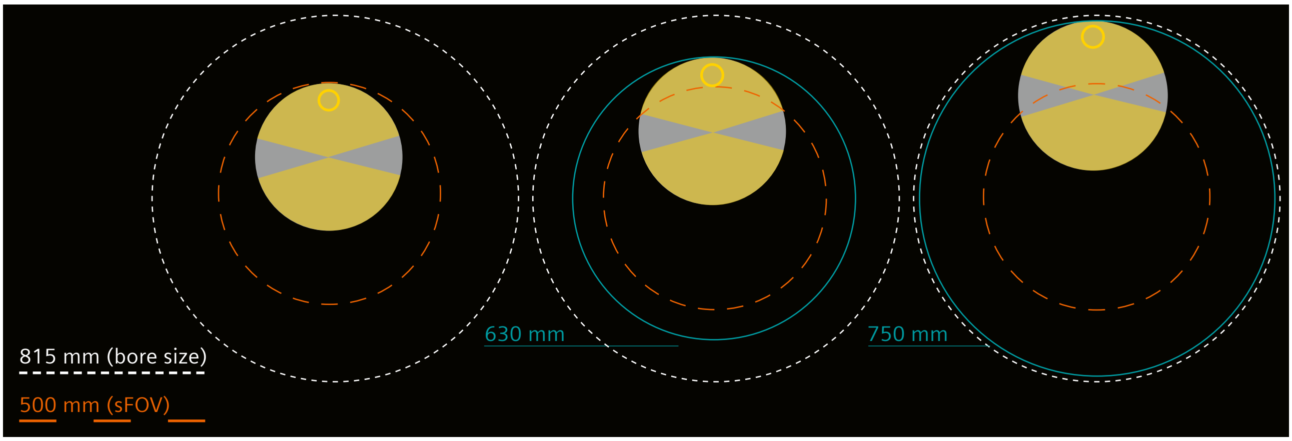

Figure 6: Measurement setup on the 82-cm-bore CT scanners SOMATOM X.cite and NAEOTOM Alpha. Phantom positions were adjusted to the bore size of the scanner. The 75 line profiles in the six central slices were used to report the accuracy of the phantom diameter.

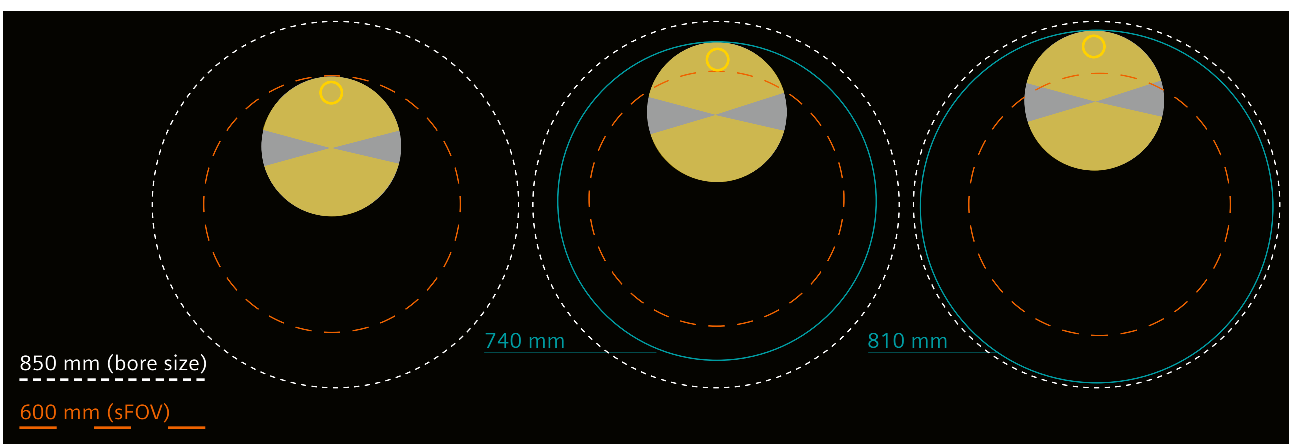

Figure 7: Measurement setup on the 85-cm-bore CT scanner SOMATOM go.Open Pro. Phantom positions were adjusted to the bore size of the CT scanner. The 75 line profiles in the six central slices were used to report the accuracy of the phantom diameter.

Results and discussion

HU accuracy

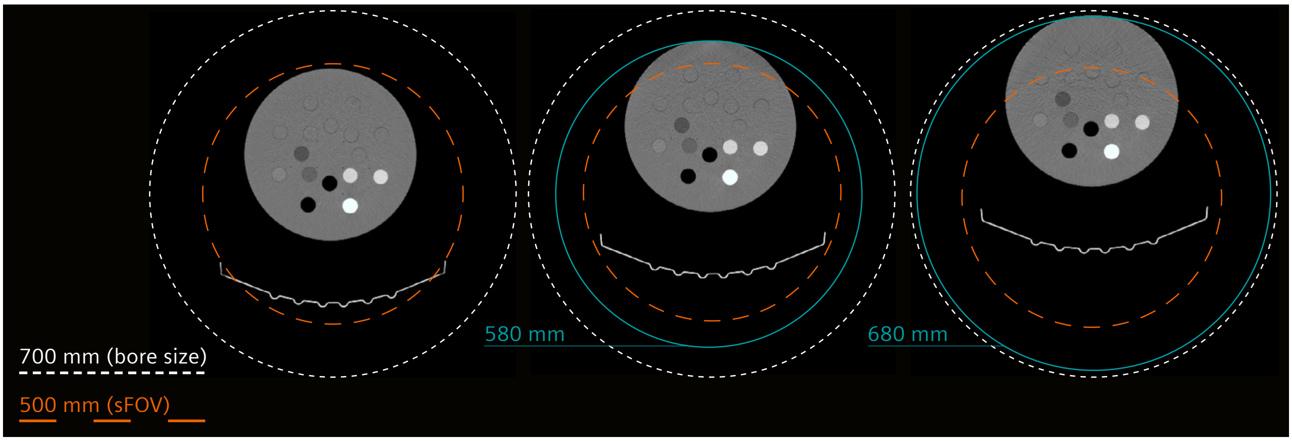

Figure 8: Measurement setup on the 70-cm-bore CT scanner SOMATOM go.Up. Phantom positions were adjusted to the bore size of the CT scanner. The 75 line profiles in the six central slices were used to report the accuracy of the phantom diameter.

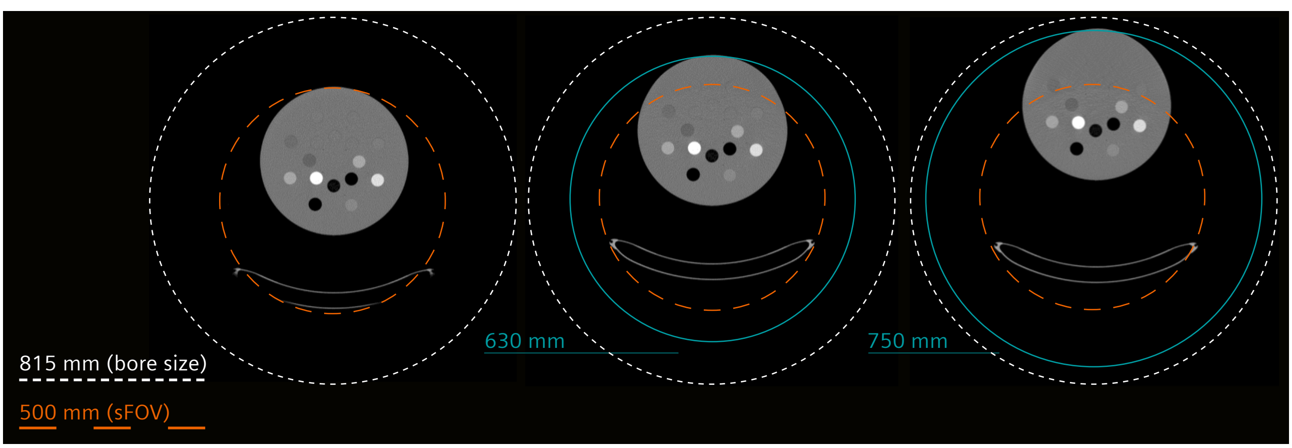

Figure 9: Results from SOMATOM X.cite. Gammex phantom reconstructed at different positions. From left to right: phantom completely in the sFOV, outer phantom edge at approximately 630 mm, and outer phantom edge at approximately 750 mm.

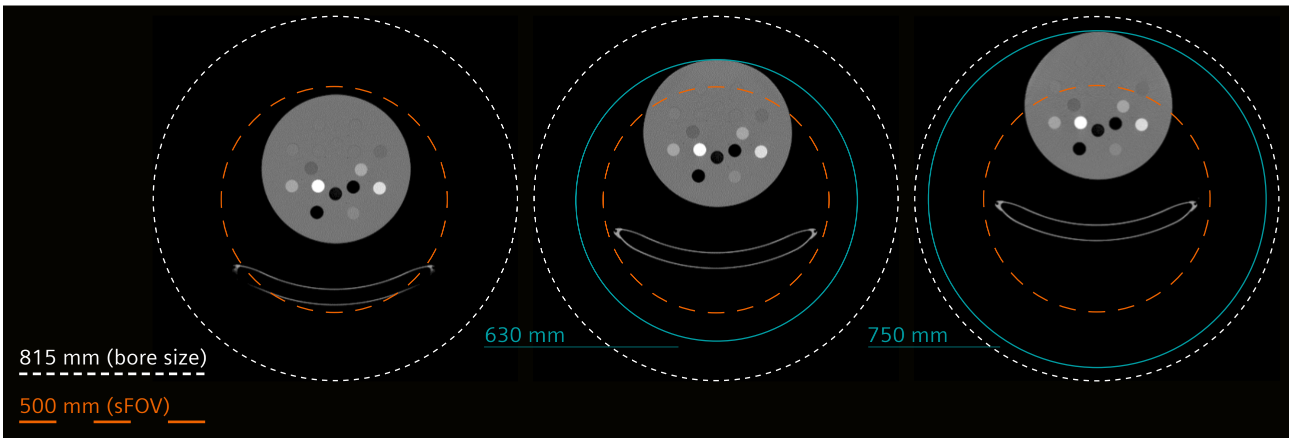

Figure 10: Results from NAEOTOM Alpha. Gammex phantom reconstructed at different positions. From left to right: phantom completely in the sFOV, outer phantom edge at approximately 630 mm, and outer phantom edge at approximately 750 mm.

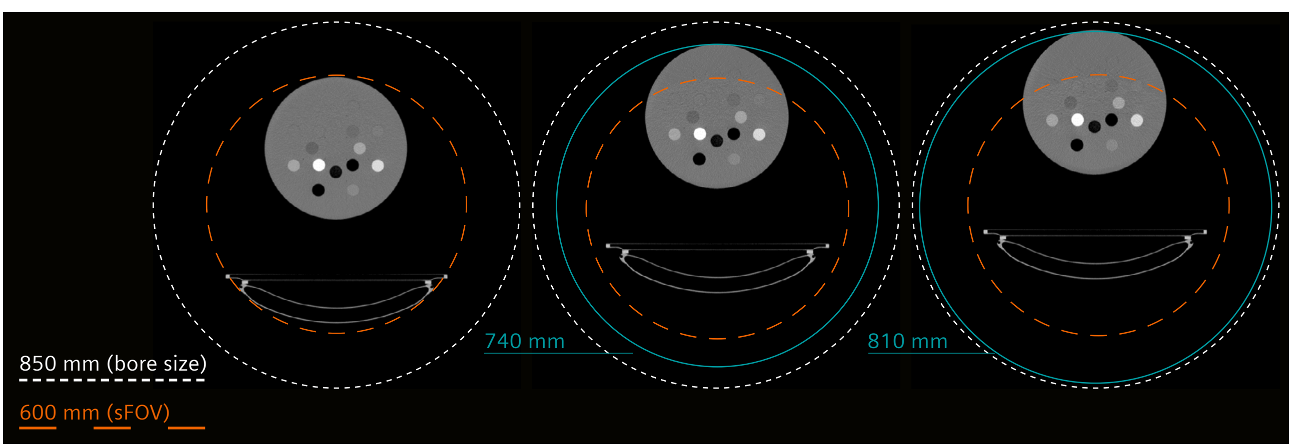

Figure 11: Results from SOMATOM go.Open Pro. Gammex phantom reconstructed at different positions. From left to right: phantom completely in the sFOV, outer phantom edge at approximately 740 mm, and outer phantom edge at approximately 810 mm.

Measurement of the mean HU values within the ROI was performed in the six central slices. Table 2 shows the average of these measurements for the different phantom positions: contained within the sFOV, phantom edge at Position 2 (Table 1) and phantom edge at Position 3 (Table 1).

Position	SOMATOM go.Up $HU_{ROI} - HU_{ROI\_Reference}$	SOMATOM X.cite $HU_{ROI} - HU_{ROI\_Reference}$	NAEOTOM Alpha $HU_{ROI} - HU_{ROI\_Reference}$	SOMATOM go.Open Pro $HU_{ROI} - HU_{ROI\_Reference}$
Position 1 (sFOV)	0.0 HU	0.00 HU	0.00 HU	0.00 HU
Position 2	8.7 HU	9.9 HU	–17.9 HU	15.9 HU
Position 3	2.7 HU	22.5 HU	–0.7 HU	13.3 HU

Table 2: HU values measured in an ROI (averaged over six central slices) at different phantom positions: phantom completely in the sFOV, a small part of the phantom outside the sFOV, and a large part of the phantom outside the sFOV.

Phantom diameter accuracy

Mean phantom diameter was measured as the average diameter from 75 line profiles for the six central image slices. The case where the entire phantom was contained within the sFOV was used as reference.

The results show that the accuracy of the diameter measurement is about 3 mm (Table 3). The results in this phantom setup imply that HD FOV 4.0 produces a consistent phantom geometry even in cases where large parts of the phantom lie outside the sFOV of the CT scanner.

Position	SOMATOM go.Up Diff. to reference diameter	SOMATOM X.cite Diff. to reference diameter	NAEOTOM Alpha Diff. to reference diameter	SOMATOM go.Open Pro Diff. to reference diameter
Position 1 (sFOV)	0.0 mm	0.00 mm	0.00 mm	0.00 mm
Position 2	–0.67 mm	–1.35 mm	0.80 mm	–1.58 mm
Position 3	0.36 mm	–2.40 mm	1.79 mm	–1.69 mm

Table 3: Mean diameter deviation of the Gammex phantom measured in six central slices.
Difference to the reference (phantom completely within the sFOV) is used to estimate diameter accuracy.

Known limitations

The HD FOV 4.0 algorithm is designed to estimate data in regions that were not covered during the measurement. To do so, the algorithm uses the principle of mass conservation in projection data. This principle holds true only in the case of a 2D data acquisition in fan- or parallel-beam geometry. CT scanners from Siemens Healthineers have a cone-beam geometry and typically use a 3D spiral scan mode for data acquisition. This violates the principle of mass conservation in projection data, which is only approximately true for spiral cone-beam CT. This is a known limitation of HD FOV 4.0 and may cause artifacts in reconstructed images. Further, due to its design, the algorithm is prone to artifacts in cases where low density regions are located at the border of the sFOV and if those regions are followed by regions with a higher density further out – e.g., when the border of the sFOV lies in the patient's lung. As described in the section on mass-conserving boundary estimation, the algorithm attaches the extrapolated data smoothly to the measured data. If the border of the sFOV is in the lung region, true projection data outside the sFOV would increase again once the thorax wall and the ribs are reached. This shape of the projection data cannot always be accurately reproduced by the algorithm, and HD FOV 4.0 is currently known to be prone to artifacts in these situations. A similar effect can occur when high-density objects are located at the edge of the sFOV. Even in this case, the extended projection data is attached smoothly to the measured projections. Typically, the high-density region, e.g., a bone, is followed by lower density tissue, e.g., soft tissue or fat, which causes a discontinuity in the real projection data, which may not be sufficiently reproduced by the extrapolation. As a result, the final reconstructed image may show artifacts.

For correcting a given projection at a certain view angle, HD FOV 4.0 needs the data from prior projections: If the scanned patient changes dramatically in z direction, this may lead to artifacts. This is even more of an issue for phantom scans, when phantoms that are quite short (relative to the detector width) in z direction are scanned in spiral mode. The transition from air to phantom, and the short phantom length, cause artifacts in HD FOV 4.0 reconstructions.

When using HD FOV 4.0, one should always be aware that the algorithm estimates data where no data were measured. Therefore, the regions beyond the border of the sFOV are only an educated guess of the real patient shape and HU values. Inside the sFOV, all data needed for the reconstruction were measured during the scan, and images resemble the patient anatomy correctly – as in standard non-HD FOV reconstructions. Outside the sFOV, data is at least partly estimated by HD FOV 4.0.

Conclusion

The HD FOV 4.0 algorithm improves upon the earlier generations of extended FOV algorithms in CT scanners from Siemens Healthineers. It supports image reconstruction while improving the visualization of anatomy in the regions outside an sFOV of 50 cm for 60 cm. In the phantom study, an HU value accuracy of about ± 40 HU was achieved with a skin-line accuracy of about ± 3 mm.

References

[1] Gysbrechts, S; Scheelen, I; and Bruder, H. HD Field of View in Computed Tomography for RT Planning: Whitepaper. Siemens Healthcare; 2012.

[2] Gersh, J; and Mistry, N. Evaluating the Evolution of Extended Field of View Algorithms in CT Simulators from Siemens Healthineers: Whitepaper, Siemens Medical Solutions USA, Inc., 2017.

[3] https://cspmedical.com/content/102-1492_tissue_phantom_user_guide.pdf

The products/features mentioned herein
are not commercially available in all countries.
Their future availability cannot be guaranteed.

Siemens Healthineers Headquarters
Siemens Healthineers AG
Siemensstr. 3
91301 Forchheim, Germany
Phone: +49 9191 180
siemens-healthineers.com

Published by Siemens Healthineers AG · 15953 0125 online ·